

# Nonlinear dynamics of plasma oscillations modeled by a forced modified Van der Pol-Duffing oscillator

C. H. Miwadinou\*, L. A. Hinvi<sup>†</sup>, A. V. Monwanou<sup>‡</sup> and  
J. B. Chabi Orou<sup>§</sup>

## Abstract

This paper considers nonlinear dynamics of plasma oscillations modeled by a forced modified Van der Pol-Duffing oscillator. These plasma oscillations are described by a nonlinear differential equation of the form  $\ddot{x} + \epsilon(1 + x^2)\dot{x} + x + \epsilon\alpha x\dot{x} + \beta x^2 + \gamma x^3 = F \cos \Omega t$ . The amplitudes of the forced harmonic, superharmonic and subharmonic oscillatory states are obtained using the harmonic balance technique and the multiple time scales methods. Admissible values of the amplitude of the external strength are derived. Bifurcation sequences displayed by the model for each type of oscillatory states are performed numerically through the fourth order Runge-Kutta scheme.

## 1 Introduction

Many problems in physics, chemistry, biology, etc., are related to nonlinear self-excited oscillators [24]. Interests according to plasma oscillations are due to their potential applications. Indeed, radio-wave propagation in the ionosphere was an early stimulus for the development of the theory of plasma. Nowadays, plasma processing is viewed as critical technology in a large number of industries. It is also important in other sectors such as biomedecine, automobiles, defence, aerospace, optics, solar energy, telecommunications, textiles, papers, polymers and waste management [25]. For example, in particular, the nonlinear description of

---

\*clement.miwadinou@imsp-uac.org, hodevewan@yahoo.fr

<sup>†</sup>laurent.hinvi@imsp-uac.org

<sup>‡</sup>movins2008@yahoo.fr

<sup>§</sup>Author to whom correspondence should be addressed: jchabi@yahoo.fr

plasma oscillations is of interest as a result of its importance to the semiconductor industry[8], [9]. Experiments suggest that some plasma behavior is approximately described by anharmonic oscillations. Thus, it has been shown experimentally [10] and theoretically [11] that in plasma physics, the electron beam surfaces, the Tonks-Datter resonances of mercury vapor and low frequency ion sound waves, oscillations are described by the following anharmonic equations (1) or (2) [12].

$$\ddot{x} + \omega_0^2 x + \beta x^2 + \gamma x^3 = F \cos \Omega t; \quad (1)$$

$$\ddot{x} + \epsilon (1 + x^2) \dot{x} + \omega_0^2 x + \beta x^2 + \gamma x^3 = F \cos \Omega t. \quad (2)$$

In these equations,  $\omega_0$  and  $\Omega$  are respectively the natural and external frequencies.  $F$  stands for the amplitude of the external excitation while  $\beta, \gamma$  and  $\epsilon$  are the quadratic, cubic nonlinearities and dampind parameters. In [11], the authors studied the regular and chaotic behaviors of plasma oscillations. In [12], the authors studied with a rigorous theoretical consideration that through a method based on the harmonic-balance formalism the amplitude of the forced harmonic oscillations states. It is found also the resonance states and admissible values of  $F$  and bifurcation structures are numerically found. They confirmed this prediction with numerical simulations and the important effects of differents parameters.

In the present paper, we concentrate our studies on the model and equation of motion, the resonant states, the chaotic behavior. Through these studies, we found the effects of differents parameters in general and in particular on the effect of the hybride quadratic parameter  $\alpha$  which shown the difference between this equation and anharmonic equation which obtained in [12].

The paper is structured as follows: Section 2 gives the model and equation of nonlinear dynamics of plasma oscillations. Section 3 gives an analytical treatment of equation (22). Amplitude of the forced harmonic oscillatory states is obtained with harmonic-balance method [1]. Section 4 investigate using multiple time-scales method [2] the resonant cases and the stability conditions are found by the perturbation method [1]. The section ends evaluates bifurcation and chaotic behavior by numerically simulations of equation (22). Section 6 deals with conclusions.

## 2 MODEL AND EQUATION OF MOTION

We consider the two-fluid model which treats the plasma as two inter penetrating conducting fluids. This model consists of a set of fluid equations for the electrons and ions plus the complete set of Maxwell's equations. Such a model has

been source of growing interest for researchers for many years [13] to [15] and nowadays, it remains an interesting task because of its potential applications[16] to [20]. The two-fluid plasma system is applicable in many areas where high density plasmas interact with high frequency electromagnetic waves. A few examples include application to helicon thrusters, electron cyclotron resonance plasma sources and plasmas resulting from strong explosions in the atmosphere. In the electrostatic situation it also has possible application in modeling discharge cathode plasma sources which are important in ion thrusters and hall thrusters. The Eulerian equations of motion in electric and magnetic fields  $E$ ,  $B$  are given as follows [21]:

$$n_0 M_\alpha \frac{dv_\alpha}{d\tau} = n_0 e (E + v_\alpha \wedge B_0 - \eta J) - \nabla P_\alpha, \quad (3)$$

$$\frac{\partial n_\alpha}{\partial \tau} + \nabla \cdot (n_0 v_\alpha) = S \quad (4)$$

$$\frac{d}{d\tau} (P_\alpha n_\alpha^{-\gamma}) = 0. \quad (5)$$

$S$  is the source term due to ionization or to large amplitude oscillations present in the plasma. The suffix " $\alpha$ " stands for the species label and it will be denoted by  $i$  and  $e$  respectively for positive ions with charge  $+e$  and electron with charge  $-e$ .  $n_\alpha$  stands for the density of the species,  $v_\alpha$  their velocity,  $P_\alpha$  their pressure,  $\gamma$  the usual specific heat ratio and  $\eta$  the resistive collision which is defined as

$$\eta = \frac{M v_\alpha}{n e^2}, \quad (6)$$

where  $\nu_\alpha$  is the collision frequency of the species  $\alpha$ . The electric charge density  $\rho$  and current  $J$  are given by

$$\rho = \sum_\alpha n_\alpha q_\alpha, J = \sum_\alpha n_\alpha q_\alpha v_\alpha. \quad (7)$$

These quantities are the source terms for Maxwell's equations. In order to deal with small amplitude waves, we consider a "background" situation representing uniform infinite plasma. The values of  $n_\alpha$ ,  $v_\alpha$ ,  $P_\alpha$ ,  $E$ ,  $B$  for this will be denoted by  $n_{0\alpha}$ , etc; however, here we shall take  $v_\alpha = E = 0$  in the unperturbed state. We then have  $J = 0$  and all of Eqs.(3)-(7) are satisfied except Eqs. (7) which require  $\rho = 0$ , hence

$$\sum_\alpha n_\alpha q_\alpha = 0. \quad (8)$$

For our simple two-species plasma, that condition of charge neutrality becomes

$$n_{0e} = n_{0i} = n_0.$$

We now consider the  $M_e = 0$  ion-sound instability and introduce perturbations terms which are denoted by the suffix 1, namely

$$n_i = n_0 + n_1, P_i = P_0 + P_1, B_i = B_0 + B_1 \quad (9)$$

Let us note that for other variables which vanish at the unperturbed state, labels 0 and 1 are not necessary.  $n_1$  is considered as a perturbed time varying function of  $z$ . We then insert the expressions (9) into Eqs. (3)-(5) and after all of the second order perturbation terms have been discarded, we obtain the following equations.

$$n_0 M_i \frac{dv_i}{d\tau} = n_0 e (E + v_i \wedge B_0 - \eta J) - \nabla P_1, \quad (10)$$

$$\frac{\partial n_1}{\partial \tau} + \nabla \cdot (n_0 v_i) = S \quad (11)$$

$$\frac{P_1}{p_0} = \gamma \frac{n_1}{n_0} \quad (12)$$

Since in this case of the ion-sound instability under consideration, only spatial variation of the form  $e^{-jk_z z}$  ( $j$  is a complex number) needs to be considered [14]. Here,  $k_z$  stands for the wave number in the  $z$  direction. In dealing with Eq.(5) and taking each species to be a perfect gas with unperturbed temperature  $T$  (which could be different for each species), we have

$$P_0 = n_0 k_B T_i, \quad (13)$$

where  $k_B$  is Boltzmann's constant and Eq. (10) can be rewritten as follows:

$$n_0 M_i \frac{dv_i}{d\tau} = n_0 e (E + v_i \wedge B_0 - \eta J) - \gamma k_B T_i \nabla n_1. \quad (14)$$

To investigate the two-fluid model, we assume that

$$E = -\nabla \phi, \quad (15)$$

where  $\phi$  is the corresponding potential and consider the Boltzmann distribution equation of electron given as follow:

$$\frac{n_1}{n_0} = \frac{e\phi}{k_B T_e} \quad (16)$$

By considering

$$\frac{dv_i}{d\tau} = \frac{\partial v_i}{\partial \tau} + (v_i \cdot \nabla) v_i, \quad (17)$$

eliminating  $v_i$  between Eqs.(4) and (14), we obtain after some algebraic manipulations the following equation

$$\begin{aligned} \frac{d^2 n_1}{d\tau^2} - \frac{k_B}{M_i} (T_e + \gamma T_i) \nabla^2 n_1 + \frac{n_0 e}{M_i} \nabla \cdot (v_i \wedge B_0) + \\ - \nu_i \left( S - \frac{\partial n_1}{\partial \tau} \right) - \frac{dS}{d\tau} = 0. \end{aligned} \quad (18)$$

Keen and Fletcher[13], [14] and Hsuan [21] in the early seventies showed that from thermodynamics argument, the source term is a function of density  $n_1$ .

Here, the source is taken to be of the following form

$$S = -\lambda n_1^2 - \mu n_1^3, \quad (19)$$

By assuming that the model is influenced by an external sinusoidal excitation  $F_0 \cos \omega \tau$ , Eq.(18) becomes

$$\begin{aligned} \frac{d^2 n_1}{d\tau^2} + (\nu_i + 2\lambda n_1 + 3\mu n_1^2) \frac{dn_1}{d\tau} + \frac{k_B}{M_i} (T_e + \gamma T_i) \vec{k}^2 n_1 \\ - j \frac{n_0 e}{M_i} \vec{k} \cdot (v_i \wedge B_0) + \nu_i (\lambda n_1^2 + \mu n_1^3) = F_0 \cos \omega \tau \end{aligned} \quad (20)$$

where  $\nabla = -j\vec{k}$ .

If one considers the slab geometry configuration for which density varies in the  $x$ -direction and the  $z$ -axis coincides with the magnetic field direction, (20) takes the following expression

$$\begin{aligned} \frac{d^2 n_1}{d\tau^2} + (\nu_i + 2\lambda n_1 + 3\mu n_1^2) \frac{dn_1}{d\tau} + \omega_0^2 n_1 + \nu_i (\lambda n_1^2 + \mu n_1^3) = \\ F_0 \cos \omega \tau; \end{aligned} \quad (21)$$

Following the rescaling

$$\omega_0 = k_z C_K, C_K = \sqrt{k_B \left( \frac{T_e + \gamma T_i}{M_i} \right)}, t = \tau \omega_0, n_1 = \left( \frac{\nu_i}{3\mu} \right)^{1/2} x = Ax, F = \frac{F_0}{A \omega_0^2}, \Omega = \frac{\omega}{\omega_0}.$$

It comes that the system is governed by the following nonlinear second order differential anharmonic equation

$$\ddot{x} + \epsilon (1 + x^2) \dot{x} + x + \epsilon \alpha x \dot{x} + \beta x^2 + \gamma x^3 = F \cos \Omega t; \quad (22)$$

$$\text{with: } \epsilon = \frac{\nu_i}{\omega_0}, \alpha = \frac{2\lambda}{\nu_i} \left( \frac{\nu_i}{3\mu} \right)^{1/2}, \beta = \frac{\lambda \nu_i}{\omega_0^2} A = \frac{\lambda \nu_i}{\omega_0^2} \left( \frac{\nu_i}{3\mu} \right)^{1/2}, \gamma = \frac{\mu \nu_i}{\omega_0^2} A^2 = \frac{\mu \nu_i}{\omega_0^2} \frac{\nu_i}{3\mu}.$$

This equation (22) is a forced modified Van der Pol-Duffing oscillator equation. There is the equation that modeled the non linear dynamics oscillators of the plasma. There are several physical mechanisms that could mimic the driven force  $F$ . For example, the transport of dust particles into plasma is proportional to the dust charge and as well as to the coagulation of small particles into larger ones since charged particles attract or repel each other through the coulomb potential. But, considering the fact that ultraviolet light can extract electrons from materials by photo-detachment, such a light can be used as an external force to control the charge on a dust particle [22]. Such forcing terms could also be mimicked through an externally applied electric field that supplies the system with an external drive[16]. In particular when the friction term vanish ( $\epsilon = 0$ ), then the equation reduces to forced modified Duffing oscillator equation studies by H. G. Engieu Kadji and al.(2005). When  $\epsilon \neq 0$  and  $\alpha = 0$ , the equation (22) reduces to an anharmonic oscillator, study two yields ago by H. G. Engieu Kadji and al.(2007)[12]. It should be quoted that the coefficient of the dissipation term plays a key role on how a limit cycle is born and how it dies. Additionally, non dissipative plasma that corresponds to the ideal case has been mainly considered in the two-fluid stationary states studies for many decades. But, since the plasma is dissipative and externally driven in realistic experimental situations, it is of interest to elaborate a formalism for investigating the driven dissipative two-fluid model in order to forecast theoretical results closer to those of the experiments. We will also see the condition of Hopf bifurcation apparition. We will finally study the transition to chaos of the system.

### 3 AMPLITUDE OF THE FORCED HARMONIC OSCILLATORY STATES

Assuming that the fundamental component of the solution and the external excitation have the same period, the amplitude of harmonic oscillations can be tackled using the harmonic balance method [1]. For this purpose, we express its solutions as

$$x = A \cos(\Omega - \psi) t + \xi \quad (23)$$

where  $A$  represents the amplitude of the oscillations and  $\xi$  a constant. Inserting this solution (23) in (22) and equating the constants and the coefficients of  $\sin \omega t$

and  $\cos \omega t$ , we have

$$\begin{aligned} & \left[ (1 - \Omega^2)A + 2\beta A\xi + \gamma\left(\frac{3}{4}A^3 + 3A\xi^2\right) \right]^2 = \\ & -\epsilon^2 \left[ A\Omega(1 + \alpha\xi + \xi^2) + \frac{1}{4}A^3\Omega \right]^2 + F^2, \end{aligned} \quad (24)$$

$$\left(1 + \frac{3}{2}\gamma A^2\right)\xi + \frac{1}{2}\beta A^2 + \beta\xi^2 + \gamma\xi^3 = 0. \quad (25)$$

If it is assumed that  $|\xi| \ll |A|$ , i.e that shift in  $x = 0$  is small compared to the amplitude [8], then  $\xi^2$  and  $\xi^3$  terms in (25) can be neglected and one obtains

$$\xi = -\frac{\beta A^2}{(2 + 3\gamma A^2)}. \quad (26)$$

Substituting (26) into (24) leads us to the following nonlinear algebraic equation

$$\begin{aligned} & \left[ \frac{9}{4}\gamma^2 A^5 + \left( \frac{9}{2}\gamma - 3\gamma\Omega^2 - 2\beta^2 \right) A^3 + 2(1 - \Omega^2)^2 A \right]^2 \\ & + \epsilon^2 \Omega^2 \left[ A \left( 1 + \frac{1}{4}A^2 \right) (2 + 3\gamma A^2) - \alpha\beta A^3 \right]^2 \\ & - F^2 (2 + 3\gamma A^2)^2 = 0 \end{aligned} \quad (27)$$

$\Longleftrightarrow$

$$\begin{aligned} & \frac{9}{16} (9\gamma^2 + \epsilon^2 \Omega^2) \gamma^2 A^{10} + \\ & + \left[ \frac{9}{2}\gamma^2 \left( \frac{9}{2}\gamma - 3\gamma\Omega^2 - 2\beta^2 \right) + \frac{9}{2}\epsilon^2 \Omega^2 \gamma^2 + \frac{3}{8}\epsilon^2 \gamma - \frac{3}{2}\alpha\beta\gamma\epsilon^2 \Omega \right] A^8 + \\ & + \left[ 9\gamma^2 (1 - \Omega^2) + \left( \frac{9}{2}\gamma - 3\gamma\Omega^2 - 2\beta^2 \right)^2 + 9\epsilon^2 \gamma^2 \Omega^2 + 3\epsilon^2 \gamma \Omega^2 \right] A^6 + \\ & + \left[ \frac{1}{4}\epsilon^2 \Omega^2 - 6\alpha\beta\gamma\epsilon^2 \Omega^2 - \alpha\beta\epsilon^2 \Omega^2 + \epsilon^2 \alpha^2 \beta^2 \Omega^2 \right] A^4 + \\ & + \left[ 4(1 - \Omega^2) \left( \frac{9}{2}\gamma - 3\gamma\Omega^2 - 2\beta^2 \right) \right] A^4 + \\ & + [6\epsilon^2 \Omega^2 + 6\epsilon^2 \Omega^2 \gamma - 4\alpha\beta\epsilon^2 \Omega^2 - 9\gamma^2 F^2] A^4 + \\ & + [4(1 - \Omega^2)^2 - 6\gamma F^2] A^2 - 4F^2 = 0 \end{aligned} \quad (28)$$

This equation can be rewritten as:

$$A^{10} + P_1 A^8 + P_2 A^6 + P_3 A^4 + P_4 A^2 - 4F = 0, \quad (29)$$

with

$$P_1 = \frac{\frac{9}{2}\gamma^2 \left(\frac{9}{2}\gamma - 3\gamma\Omega^2 - 2\beta^2\right) + \frac{9}{2}\epsilon^2\Omega^2\gamma^2 + \frac{3}{8}\epsilon^2\gamma - \frac{3}{2}\alpha\beta\gamma\epsilon^2\Omega}{\frac{9}{16}(9\gamma^2 + \epsilon^2\Omega^2)\gamma^2}, \quad (30)$$

$$P_2 = \frac{9\gamma^2(1 - \Omega^2) + \left(\frac{9}{2}\gamma - 3\gamma\Omega^2 - 2\beta^2\right)^2 + 9\epsilon^2\gamma^2\Omega^2 + 3\epsilon^2\gamma\Omega^2}{\frac{9}{16}(9\gamma^2 + \epsilon^2\Omega^2)\gamma^2} + \frac{\frac{1}{4}\epsilon^2\Omega^2 - 6\alpha\beta\gamma\epsilon^2\Omega^2 - \alpha\beta\epsilon^2\Omega^2 + \epsilon^2\alpha^2\beta^2\Omega^2}{\frac{9}{16}(9\gamma^2 + \epsilon^2\Omega^2)\gamma^2}, \quad (31)$$

$$P_3 = \frac{4(1 - \Omega^2)\left(\frac{9}{2}\gamma - 3\gamma\Omega^2 - 2\beta^2\right)}{\frac{9}{16}(9\gamma^2 + \epsilon^2\Omega^2)\gamma^2} + \frac{6\epsilon^2\Omega^2 + 6\epsilon^2\Omega^2\gamma - 4\alpha\beta\epsilon^2\Omega^2 - 9\gamma^2 F^2}{\frac{9}{16}(9\gamma^2 + \epsilon^2\Omega^2)\gamma^2}, \quad (32)$$

$$P_4 = \frac{4(1 - \Omega^2)^2 - 6\gamma F^2}{\frac{9}{16}(9\gamma^2 + \epsilon^2\Omega^2)\gamma^2}. \quad (33)$$

We investigate the effects of the quadratic and cubic terms on the behavior of the amplitude of plasma oscillations. The obtained results are reported in Figs. 1, 2 and 3 where the hysteresis and jump phenomena are found. It should be stressed that the hysteresis and jump phenomena known to be function of the cubic nonlinear coefficient can also be triggered or quenched through the dissipative coefficient  $\epsilon$  (see Figs. 3) and as well as via the nonlinear quadratic parameter  $\beta$  and  $\alpha$  (see Figs. 1, 2). Through (29), the behavior of the amplitude of plasma oscillations is investigated when the external frequency  $\Omega$  varies. Thereby, the observed resonant state obtained for a set of parameters can be destroyed according to the value taken by the amplitude of the external force. During the hysteresis and jump phenomena processes, for any value of the frequency  $\Omega$  and the external force  $F$  respectively, three different amplitudes of oscillations are obtained among which, two are stable and one is unstable.



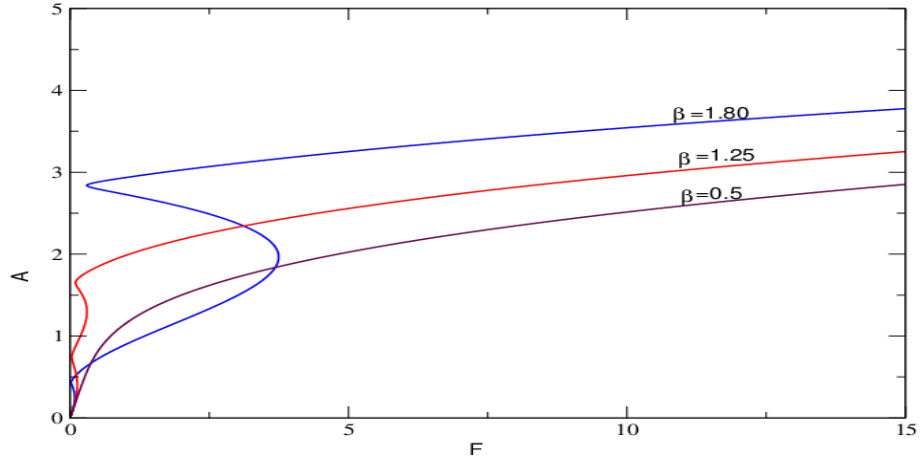


Figure 1: Effects of  $\beta$  on the amplitude-response curves with  $\Omega = 0.7; \gamma = 0; \epsilon = 0.05$  and  $\alpha = 0$ .

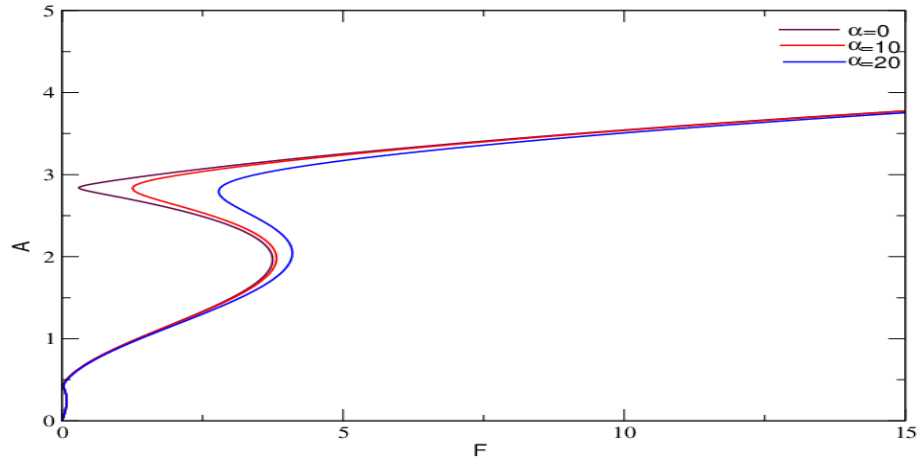


Figure 2: Effects of  $\alpha$  on the amplitude-response curves with  $\Omega = 0.7; \gamma = 0; \epsilon = 0.05$  and  $\beta = 1.85$ .

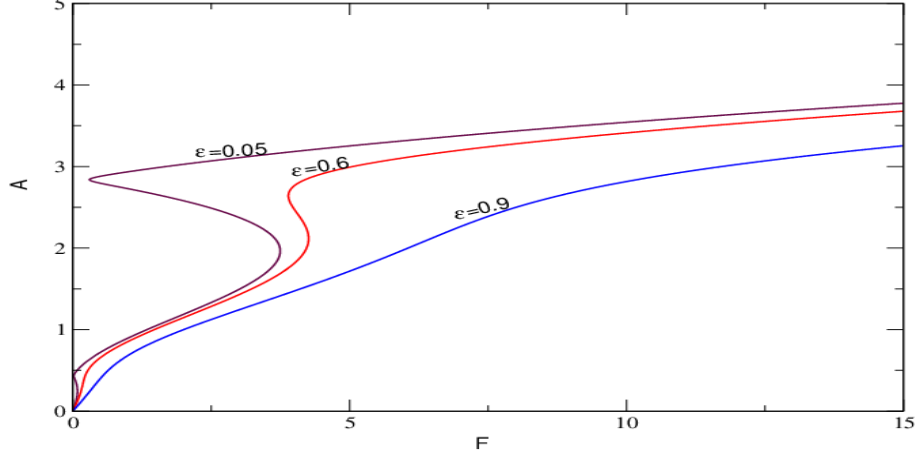


Figure 3: Effects of  $\epsilon$  on the amplitude-response curves with  $\Omega = 0.7$ ;  $\gamma = 0$ ;  $\beta = 1.85$  and  $\alpha = 0$ .

## 4 Resonant states

We investigate the different resonances with the Multiple time scales Method (*MSM*).

In such a situation, an approximate solution is generally sought as follows:

$$x(\epsilon, t) = x_0(T_0, T_1) + \epsilon x_1(T_0, T_1) + \dots \quad (34)$$

With  $T_n = \epsilon^n t$  The derivatives operators can now be rewritten as follows:

$$\frac{d}{dt} = D_0 + \epsilon D_1 + \dots \quad (35)$$

$$\frac{d^2}{dt^2} = D_0^2 + 2\epsilon D_0 D_1 + \dots \quad (36)$$

where  $D_n^m = \frac{\partial^m}{\partial T_n^m}$

### 4.1 Primary resonant state

In this state, we put that  $F = \epsilon F$ ,  $\beta = \epsilon \beta$ ,  $\gamma = \epsilon \gamma$ . The closeness between both internal and external frequencies is given by  $\Omega = 1 + \epsilon \sigma$ . Where  $\sigma$  is the detuning parameter. Inserting (36) and (37) into (22) we obtain:

$$\begin{aligned} & (D_0^2 + 2\epsilon D_0 D_1) (x_0 + \epsilon x_1) + \\ & + \epsilon [1 + (x_0 + \epsilon x_1)^2] (D_0 + \epsilon D_1) (x_0 + \epsilon x_1) + \\ & + x_0 + \epsilon x_1 + \epsilon \alpha (x_0 + \epsilon x_1) (D_0 + \epsilon D_1) (x_0 + \epsilon x_1) + \\ & + \beta (x_0 + \epsilon x_1)^2 + \gamma (x_0 + \epsilon x_1)^3 - \epsilon F \cos \Omega t = 0; \end{aligned} \quad (37)$$

Equating the the coefficients of like powers of  $\epsilon$  after some algebraic manipulations, we obtain:

In order  $\epsilon^0$ ,

$$D_0^2 x_0 + x_0 = 0 \quad (38)$$

In order  $\epsilon^1$ ,

$$D_0^2 x_1 + x_1 = F \cos \Omega t - 2D_1 D_0 x_0 - (1 + x_0^2) D_0 x_0 - \alpha x_0 D_0 x_0 - \beta x_0^2 - \gamma x_0^3. \quad (39)$$

The general solution of (38) is

$$x_0 = A(T_1) \exp(jT_0) + CC, \quad (40)$$

where  $CC$  represents the complex conjugate of the previous terms.  $A(T_1)$  is a complex function to be determined from solvability or secular conditions of (39). Thus, substituting the solution  $x_0$  in (40) leads us to the following secular criterion

$$2jA' + j(1 + |A|^2)A + 3\gamma|A|^2A - \frac{F}{2} \exp(j\sigma T_1) = 0 \quad (41)$$

In polar coordinates, the solution of (41) is

$$A = \frac{1}{2}a(T_1) \exp[j\theta(T_1)] \quad (42)$$

where  $a$  and  $\theta$  are real quantities and stand respectively for the amplitude and phase of oscillations. After injecting (42) into (41), we separate real and imaginary terms and obtain the following coupled flow for the amplitude and phase:

$$a' = -\frac{a}{2} - \frac{a^3}{8} + \frac{F}{2} \sin \Phi \quad (43)$$

$$a\Phi' = a\sigma - \frac{3\gamma a^3}{8} - \frac{F}{2} \cos \Phi. \quad (44)$$

where the prime denotes the derivative with respect to  $T_1$  and  $\Phi = \sigma T_1 - \theta$ . For the steady-state conditions ( $a' = \Phi' = 0$ ), the following nonlinear algebraic equation is obtained :

$$\left(\frac{9\gamma^2 + 1}{64}\right) a_0^6 + \left(\frac{1 - 6\gamma\sigma}{8}\right) a_0^4 + \left(\frac{1 + 4\sigma^2}{4}\right) a_0^2 - \frac{F^2}{4} = 0 \quad (45)$$

where  $a_0$  and  $\Phi_0$  are respectively the values of  $a$  and  $\Phi$  in the steady-state. Eq.(45) is the equation of primary resonance flow. Now, we study the stability of the precess, we assume that each equilibrium state is submitted to a small perturbation as follows

$$a = a_0 + a_1 \quad (46)$$

$$\Phi = \Phi_0 + \Phi_1 \quad (47)$$

where  $a_1$  and  $\Phi_1$  are slight variations. Inserting the equations (46) and (47) into (43) and (44) and canceling nonlinear terms enable us to obtain

$$a'_1 = -\frac{1}{2} \left( 1 + \frac{3a_0^2}{4} \right) a_1 - a_0 \left( \sigma - \frac{3a_0^2\gamma}{8} \right) \Phi_1 \quad (48)$$

$$\Phi'_1 = \frac{1}{a_0} \left( \sigma - \frac{9a_0^2\gamma}{8} \right) a_1 - \frac{1}{2} \left( 1 + \frac{a_0^2}{4} \right) \Phi_1. \quad (49)$$

The stability process depends on the sign of eigenvalues  $\mathcal{I}$  of the equations (48) and (49) which are given through the following characteristic equation

$$\mathcal{I}^2 + 2Q\mathcal{I} + R = 0, \quad (50)$$

where  $Q = \frac{1}{4} (a_0^2 + 2)$ ,  $R = \frac{1}{4} \left( 1 + \frac{3a_0^2}{4} \right) \left( 1 + \frac{a_0^2}{4} \right) - \left( \sigma - \frac{3a_0^2\gamma}{8} \right) \left( \sigma - \frac{9a_0^2\gamma}{8} \right)$ .

Since  $Q > 0$ , the steady-state solutions are stable if  $R > 0$  and unstable otherwise. Fig. 4 displays the amplitudes response curves obtained from (45) for different values of the parameter  $\gamma$  and one can observe that as it increases, the model goes from resonance to a hysteresis state.

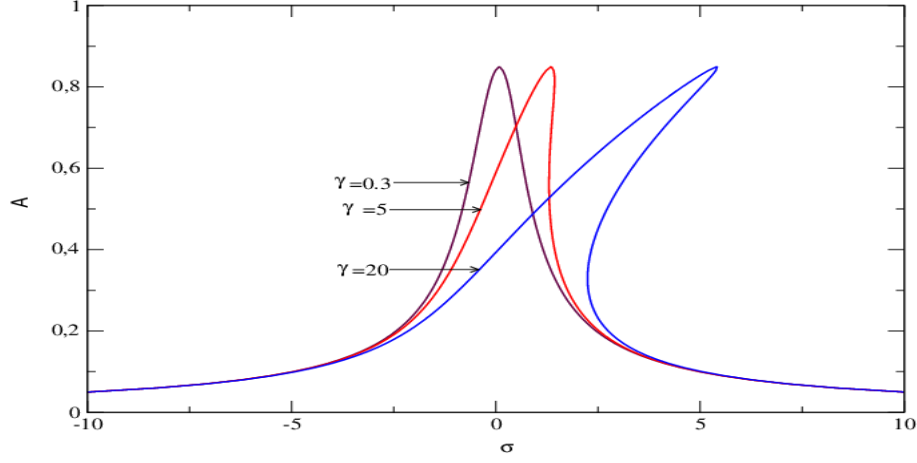


Figure 4: Effects of  $\gamma$  on the frequency-response curves of the primary resonance with the parameters for  $F = 1.0$ .

## 4.2 Superharmonic and subharmonic oscillations

When the amplitude of the sinusoidal external force is large, other type of oscillations can be displayed by the model, namely the superharmonic and the subharmonic oscillatory states. It is now assumed that  $F = \epsilon^0 F$  and therefore, one obtains the following equations at different order of  $\epsilon$ . In order  $\epsilon^0$ ,

$$D_0^2 x_0 + x_0 = F_0 \cos \Omega T_0 \quad (51)$$

In order  $\epsilon^1$ ,

$$D_0^2 x_1 + x_1 = -2D_1 D_0 x_0 - (1 + x_0^2) D_0 x_0 - \alpha x_0 D_0 x_0 - \beta x_0^2 - \gamma x_0^3. \quad (52)$$

The general solution of Eq. (52) is

$$x_0 = A(T_1) e^{jT_0} + \Lambda e^{j\Omega T_0}, \quad (53)$$

with  $\Lambda = \frac{F}{2(1-\Omega^2)}$

Substituting the general solution  $x_0$  into Eq. (53), after some algebraic manipulations, we obtain

$$\begin{aligned} D_0^2 x_1 + x_1 = & \left[ -2jA' - (j(1 + |A|^2 + 2\Lambda^2) + 3\gamma|A|^2 + 6\gamma\Lambda^2) \right] e^{jT_0} + \\ & - [j\Omega(1 + \Lambda^2 + 2|A|^2) + 3\gamma|\Lambda|^2 + 6\gamma|A|^2] \Lambda e^{j\Omega T_0} + \\ & - (j + \gamma) A^3 e^{3jT_0} - [j(1 + 2\Omega) + 3\gamma] \Lambda \Lambda^2 e^{j(1+2\Omega)T_0} + \\ & - [j(2 + \Omega) + 3\gamma] A^2 \Lambda e^{j(2+\Omega)T_0} + \end{aligned}$$

$$\begin{aligned}
& - [j(2 - \Omega) + 3\gamma] A^2 \Lambda e^{j(2-\Omega)T_0} - (j\Omega + \gamma) \Lambda^3 e^{j3\Omega T_0} + \\
& - [j(1 - 2\Omega) + 3\gamma] A \Lambda^2 e^{j(1-2\Omega)T_0} - (j\alpha + \beta) A^2 e^{2jT_0} + \\
& - (j\alpha\Omega + \beta) \Lambda^2 e^{2j\Omega T_0} - [j\alpha(1 + \Omega) + 2\beta] A \Lambda e^{j(1+\Omega)T_0} \\
& - [j\alpha(1 - \Omega) + 2\beta] A \Lambda e^{j(1-\Omega)T_0} - 2\beta (|A|^2 + \Lambda^2) + \\
& + j\alpha (|A|^2 + \Omega\Lambda^2) + CC
\end{aligned} \tag{54}$$

From Eq.(54), it comes that superharmonic and subharmonic states can be found from the quadratic and cubic nonlinearities. The cases of superharmonic oscillations we consider are  $3\Omega = 1 + \epsilon\sigma$  and  $2\Omega = 1 + \epsilon\sigma$ , while the subharmonic oscillations to be treated are  $\Omega = 3 + \epsilon\sigma$  and  $\Omega = 2 + \epsilon\sigma$ .

For the first superharmonic states  $3\Omega = 1 + \epsilon\sigma$ , equating resonant terms at 0 from Eq.(54), we obtain:

$$\begin{aligned}
& -2jA' - j(1 + |A|^2 + 2\Lambda^2)A - 3\gamma|A|^2A - 6\gamma\Lambda^2A \\
& - (j\Omega + \gamma)\Lambda^3 e^{j\epsilon\sigma T_0} = 0
\end{aligned} \tag{55}$$

Using (42) and after some algebraic manipulations, we rewrite (55) as follows

$$a' = -\frac{a}{2} - \frac{a^3}{8} - a\Lambda^2 - \Lambda^3(\Omega \cos \Phi + \gamma \sin \Phi), \tag{56}$$

$$a\Phi' = a\sigma - \frac{3\gamma a^3}{8} - 3\gamma\Lambda^2 a + \Lambda^3(\gamma \cos \Phi - \Omega \sin \Phi) \tag{57}$$

The amplitude of oscillations of this superharmonic states is governed by the following nonlinear algebraic equation

$$\begin{aligned}
& \left(\frac{a_0}{2} + \frac{a_0^3}{8} + a_0\Lambda^2\right)^2 + \left(a_0\sigma - \frac{3\gamma a_0^3}{8} - 3\gamma\Lambda^2 a_0\right)^2 - \\
& (\Omega^2 + \gamma^2)\Lambda^2 = 0.
\end{aligned} \tag{58}$$

After some algebraic manipulations, Eq.(58) can be rewritten as follows

$$\begin{aligned}
& \left(\frac{9\gamma^2 + 1}{64}\right)a_0^6 + \frac{1}{4}\left[\frac{1}{2} + \Lambda^2 - 3\gamma(\sigma - 3\gamma\Lambda^2)\right]a_0^4 = \\
& - \left[\left(\frac{1}{2} + \Lambda^2\right)^2 + (\sigma - 3\gamma\Lambda^2)^2\right]a_0^2 + (\gamma^2 + \Omega^2)\Lambda^6
\end{aligned} \tag{59}$$

and they are stable if

$$\begin{aligned}
& \frac{1}{4}\left(1 + 2\Lambda^2 + \frac{3}{4}a_0^2\right)\left(1 + 2\Lambda^2 + \frac{1}{4}a_0^2\right) + \\
& \left(\sigma - \frac{9}{8}\gamma a_0^2 - 3\gamma\Lambda^2\right)\left(\sigma - 3\gamma\Lambda^2 - \frac{3}{8}\gamma a_0\right) > 0
\end{aligned} \tag{60}$$

Fig. 5 presents the frequency response curves of the superharmonic resonance as a function of  $\sigma$  for different values of the external force. As the intensity of the external force increases, the resonance behavior observed is destroyed. The effects of the parameter  $\gamma$  on such superharmonic oscillations are also investigated and results are reported in Fig.6, showing the appearance of the hysteresis phenomenon when the nonlinear cubic parameter  $\gamma$  is increasing.

On the other hand, the second superharmonic states  $2\Omega = 1 + \epsilon\sigma$ , inserting this condition into Eq.(54) and equating the secular terms to 0, we obtain:

$$\begin{aligned} -2jA' - j(1 + |A|^2 + 2\Lambda^2)A + 3\gamma|A|^2A + 6\gamma\Lambda^2A \\ - (j\alpha\Omega + \beta)\Lambda^2e^{j\epsilon\sigma T_0} = 0 \end{aligned} \quad (61)$$

After some algebraic manipulations as in the first superharmonic resonance, we obtain:

$$\begin{aligned} \left(\frac{9\gamma^2 + 1}{64}\right)a_0^6 + \frac{1}{4}\left[\frac{1}{2} + \Lambda^2 - 3\gamma(\sigma - 3\gamma\Lambda^2)\right]a_0^4 = - \\ + \left[\left(\frac{1}{2} + \Lambda^2\right)^2 + (\sigma - 3\gamma\Lambda^2)^2\right]a_0^2 + (\alpha^2\omega^2 + \beta^2)\Lambda^6, \end{aligned} \quad (62)$$

and the stability criteria is the one defined through inequality (60). In this cases also, the influence of the quadratic parameter on such oscillations has been checked (see Figs 7 and 8). In such a state, we noticed that the peak values of this superharmonic resonance are increased progressively when increasing  $\beta$  or  $\alpha$ .

The first subharmonic oscillations ( $\Omega = 3 + \epsilon\sigma$ ) are fund. Inserting this condition into Eq.(54) and equating the secular terms to 0, we obtain:

$$\begin{aligned} -2jA' - [j(1 + |A|^2 + 2\Lambda^2) + 3\gamma|A|^2 + 6\gamma\Lambda^2]A \\ - (j(2 - \Omega) + 3\gamma)\Lambda\bar{A}^2e^{j\sigma T_0} = 0 \end{aligned} \quad (63)$$

With (42), Eq.(63) gives after some algebraic manipulations and separating real and imaginary terms,

$$a' = -\frac{a}{2} - \frac{a^3}{8} - a\Lambda^2 - \frac{1}{4}\Lambda a^2[(2 - \Omega)\cos\Phi + 3\gamma\sin\Phi], \quad (64)$$

$$a\Phi' = \frac{1}{3}a\sigma - \frac{3\gamma a^3}{8} - 3\gamma\Lambda^2a + \frac{1}{4}\Lambda a^2[3\gamma\cos\Phi - (2 - \Omega)\sin\Phi] \quad (65)$$

Study-states oscillations conditions implies

$$\begin{aligned} \left(\frac{a_0}{2} + \frac{a_0^3}{8} + a_0\Lambda^2\right)^2 + \left(\frac{1}{3}a_0\sigma - \frac{3\gamma a_0^3}{8} - 3\gamma\Lambda^2a_0\right)^2 \\ - \frac{1}{16}\Lambda^2a_0^4[(2 - \Omega)^2 + 9\gamma^2] = 0 \end{aligned} \quad (66)$$

Finally the amplitude of subharmonic oscillatory states are given by following nonlinear algebraic equation:

$$\begin{aligned} & \left( \frac{9\gamma^2 + 1}{64} \right) a_0^4 + \\ & + \left[ \frac{1}{8} + \frac{\Lambda^2}{4} - \frac{3}{4}\gamma \left( \frac{\sigma}{3} - 3\gamma\Lambda^2 \right) - \frac{1}{16}\Lambda^2 (9\gamma^2 + (2 - \Omega)^2) \right] a_0^2 + \\ & + \left[ \left( \frac{1}{2} + \Lambda^2 \right)^2 + \left( \frac{\sigma}{3} - 3\gamma\Lambda^2 \right)^2 \right] = 0 \end{aligned} \quad (67)$$

and the stability is guaranteed only if

$$\begin{aligned} & \left( \frac{1}{2} + \Lambda^2 + \frac{1}{4}a_0^2 \right) \left( \frac{1}{2} + \Lambda^2 + \frac{1}{8}a_0^2 \right) + \\ & - \left( \frac{\sigma}{9} - \gamma\Lambda^2 - \frac{1}{8}a_0^2 \right) \left( \sigma + \frac{9}{8}\gamma a_0^2 - 9\gamma\Lambda^2 \right) < 0 \end{aligned} \quad (68)$$

Now, we consider the second subharmonic oscillatory states:  $\Omega = 2 + \epsilon\sigma$ . This condition implies althrough Eq.(54) the secular term which equating 0 give

$$\begin{aligned} & -2jA' - [j(1 + |A|^2 + 2\Lambda^2) + 3\gamma|A|^2 + 6\gamma\Lambda^2] A \\ & - (j(1 - \Omega)\alpha + 2\beta) \bar{A}\Lambda e^{j\sigma T_1} = 0 \end{aligned} \quad (69)$$

We obtain that the second subharmonic oscillatory states motions are governed by the equation

$$\begin{aligned} & \left( \frac{9\gamma^2 + 1}{64} \right) a_0^4 + \\ & \left[ \frac{1}{8} + \frac{\Lambda^2}{4} - \frac{3}{4}\gamma \left( \frac{\sigma}{2} - 3\gamma\Lambda^2 \right) - \frac{1}{16}\Lambda^2 (9\gamma^2 + (2 - \Omega)^2) \right] a_0^2 + \\ & \left[ \left( \frac{1}{2} + \Lambda^2 \right)^2 + \left( \frac{\sigma}{2} - 3\gamma\Lambda^2 \right)^2 - (1 - \Omega)^2 \alpha^2 \Lambda^2 - 4\beta^2 \Lambda^2 \right] = 0 \end{aligned} \quad (70)$$

They are stable if the following criterion is fulfilled

$$\left( \frac{1}{2} + 2\Lambda^2 + \frac{1}{4}a_0^2 \right) a_0^2 + 6 \left[ \left( \frac{\sigma}{2} - 3\gamma\Lambda^2 \right) a_0^2 - \frac{3}{8}\gamma a_0^4 \right] > 0 \quad (71)$$



The frequency response curves of both types of subharmonic oscillations are plotted in Figs.9 and 10 and the regions where such behaviors occur are obtained. From these pictures, it comes that the range of frequency where a response can be obtained is more important in the first subharmonic state than in the other cases.

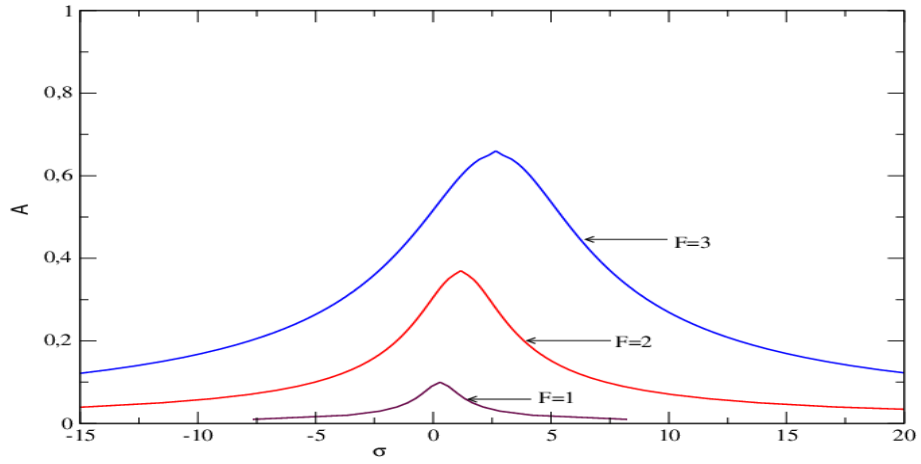


Figure 5: Effects of  $F$  on the frequency-response curves of the order-three superharmonic resonance with  $\gamma = 0.3$

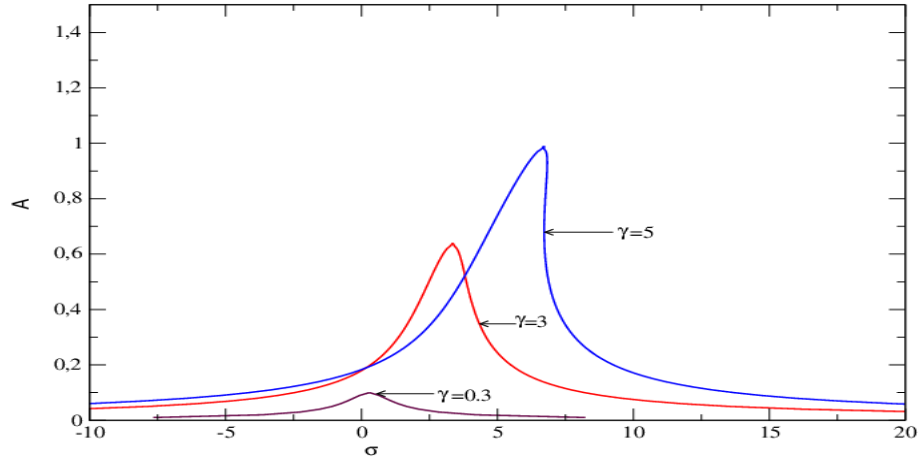


Figure 6: Effects of  $\gamma$  on the frequency-response curves of the order-three super-harmonic resonance with  $F = 1$ .

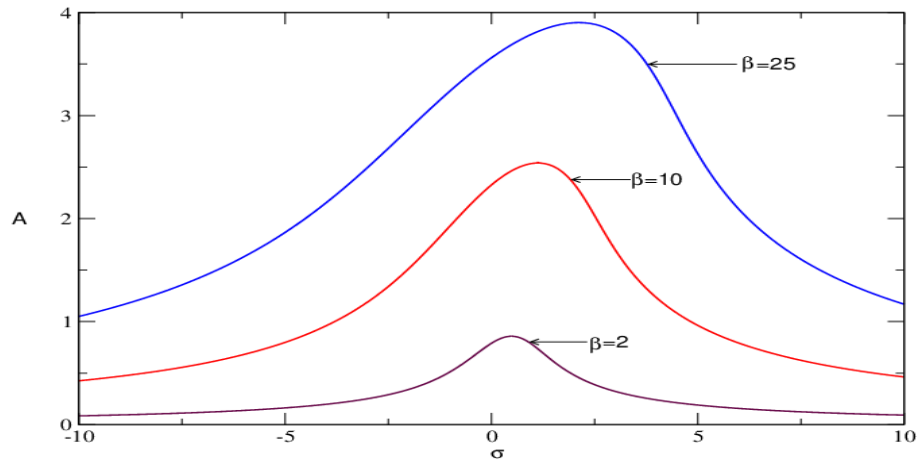


Figure 7: Effects of  $\beta$  on the frequency-response curves of the order-two super-harmonic resonance with  $F = 1$ .

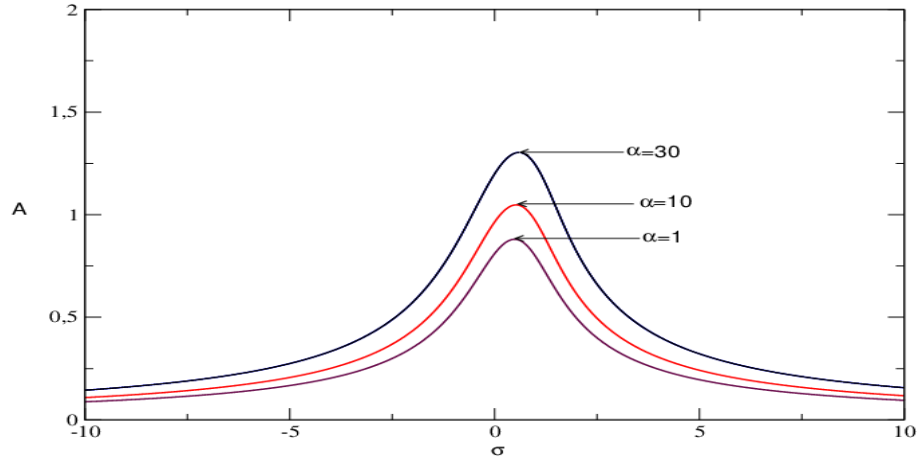


Figure 8: Effects of  $\alpha$  on the frequency-response curves of the order-two super-harmonic resonance with  $F = 1$  and  $\beta = 2$ .

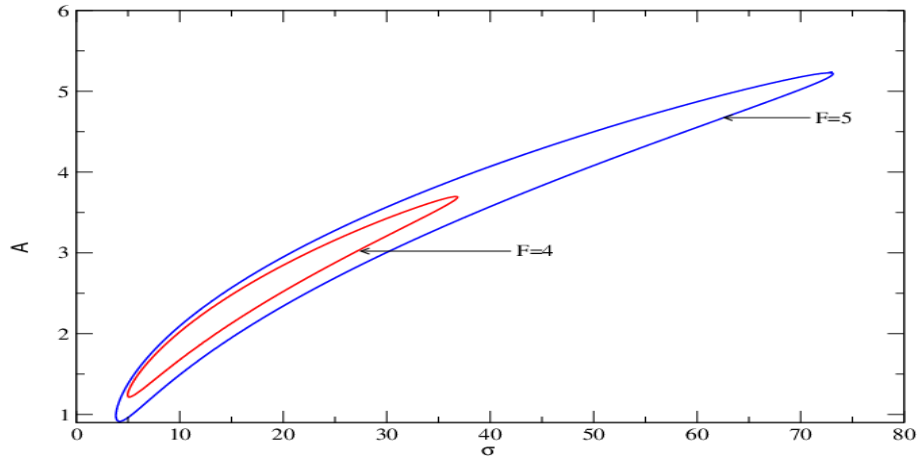


Figure 9: Effects of  $F$  on the frequency-response curves of the order-three sub-harmonic resonance with  $\gamma = 2.30$ .

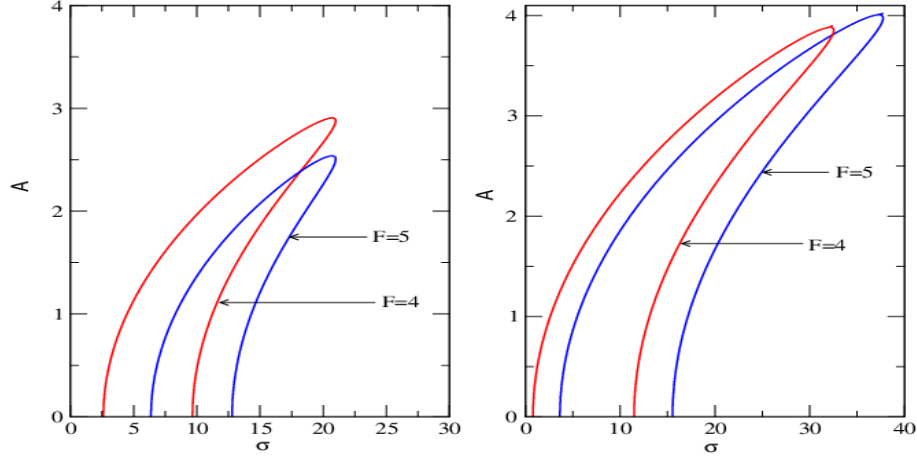


Figure 10: Effects of  $F$  on the frequency-response curves of the first subharmonic resonance with  $\gamma = 2.30$ ;  $\beta = 1$ ; left  $\alpha = 0$  and right  $\alpha = 1$ .

## 5 Bifurcation and Chaotic behavior

The aim of this section is to find some bifurcation structures in the nonlinear dynamics of plasma oscillations described by equation (22) for resonant states since they are of interest in this system. For this purpose, we numerically solve this equation using the fourth-order Runge Kutta algorithm [26] and plot the resulting bifurcation diagrams and the variation of the corresponding largest Lyapunov exponent as the amplitude  $F$ , the parameters of nonlinearity  $\epsilon$ ,  $\alpha$ ,  $\beta$  and  $\gamma$  are varied. The stroboscopic time period used to map various transitions which appear in the model is  $T = \frac{2\pi}{\Omega}$ .

The largest Lyapunov exponent which is used here as the instrument to measure the rate of chaos in the system is defined as

$$Lya = \lim_{t \rightarrow \infty} \frac{\ln \sqrt{dx^2 + d\dot{x}^2}}{t} \quad (72)$$

where  $dx$  and  $d\dot{x}$  are respectively the variations of  $x$  and  $\dot{x}$ . Initial condition that we are used in the simulations of this section is  $(x_0, \dot{x}_0) = (1, 1)$ . For the set of parameters  $\beta = 3.05$ ,  $\gamma = 1.5$ ,  $\epsilon = 0.02$ ,  $\Omega = 1$ , with  $\alpha = 0$  (left) and  $\alpha = 1$  (right) the bifurcation diagram and its corresponding Lyapunov exponent are plotted in Fig. 11. The same simulation are found in Fig.12 and Fig. 13 with respectively  $\beta = 6$  and  $\beta = 1.80$ ;  $\epsilon = 0.06$ . From the bifurcation diagrams, various types of motions are displayed. It is found that the model can switch from periodic to quasi-periodic oscillations or chaotic motions see Fig.11. In order to illustrate such situations, we have represented the various phase portraits using the

parameters of the bifurcation diagram for which periodic, quasi-periodic oscillations and chaotic motions are observed in Fig. 14 with effect of parameter  $\alpha$  in Fig.15. These observations prove that the model is highly to the initial conditions. It should be emphasized from Fig.11 that there are some domains where the Lyapunov exponent does not match very well the regime of oscillations expected from the bifurcation diagram. Far from being an error which has occurred from the numerical simulation process, such a behavior corresponds to what is called the intermittency phenomenon. Therefore, within these intermittent domains, the dynamics of the model can not be predicted. For instance, some forecasted period-1 and quasiperiodic motions from the bifurcation diagram are not confirmed by the Lyapunov exponent. From Figs. 14 and 15, it is clearly that when the quadratic hybrid parameter the chaotic as well the ones of intermittency remain in the system. On the other hand, the parameters of nonlinearity can influence the chaotic motion in model. Consequently a set of physical parameters of the model,  $\alpha, \beta, \epsilon$  and  $\gamma$  can be used to increase or dismiss the rate of chaotic motion in the model. The same simulations are obtained in the subharmonic and superharmonic resonance have also been represented respectively in Figs. 16 - 23. From these figures, we conclude that chaos is more abundant in subharmonic resonant states than in the superharmonic and primary resonances.

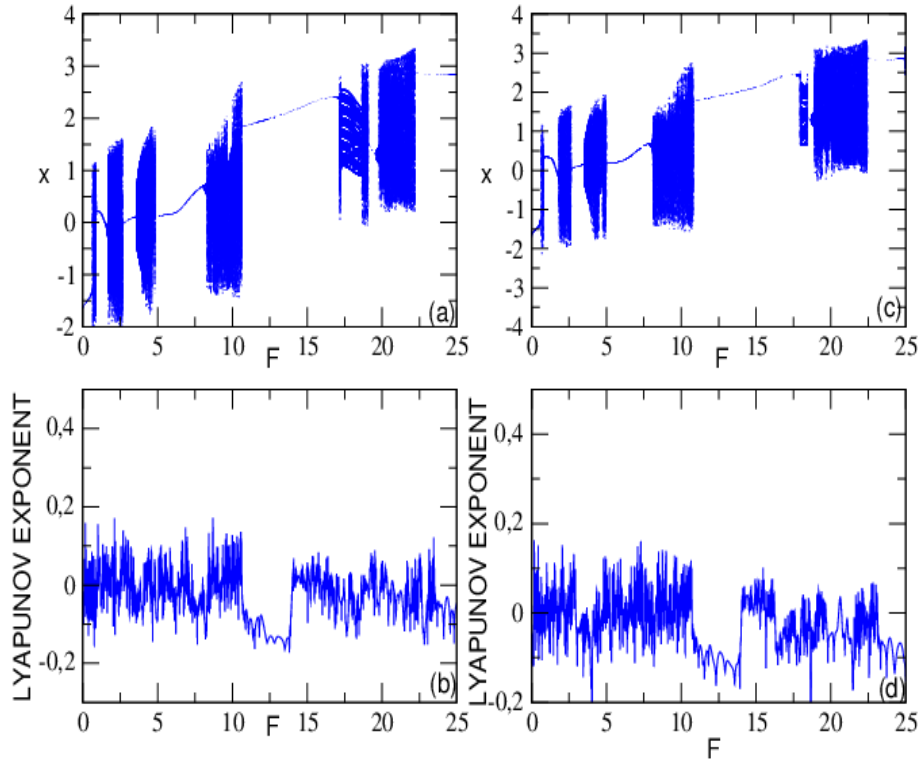


Figure 11: Bifurcation diagram (upper frame) and Lyapunov exponent (lower frame) versus the amplitude  $F$  with the parameters  $\beta = 3.05$ ;  $\gamma = 1.5$ ;  $\Omega = 1$ ;  $\epsilon = 0.02$ ;  $\alpha = 0$  (left) and  $\alpha = 1$  (right).

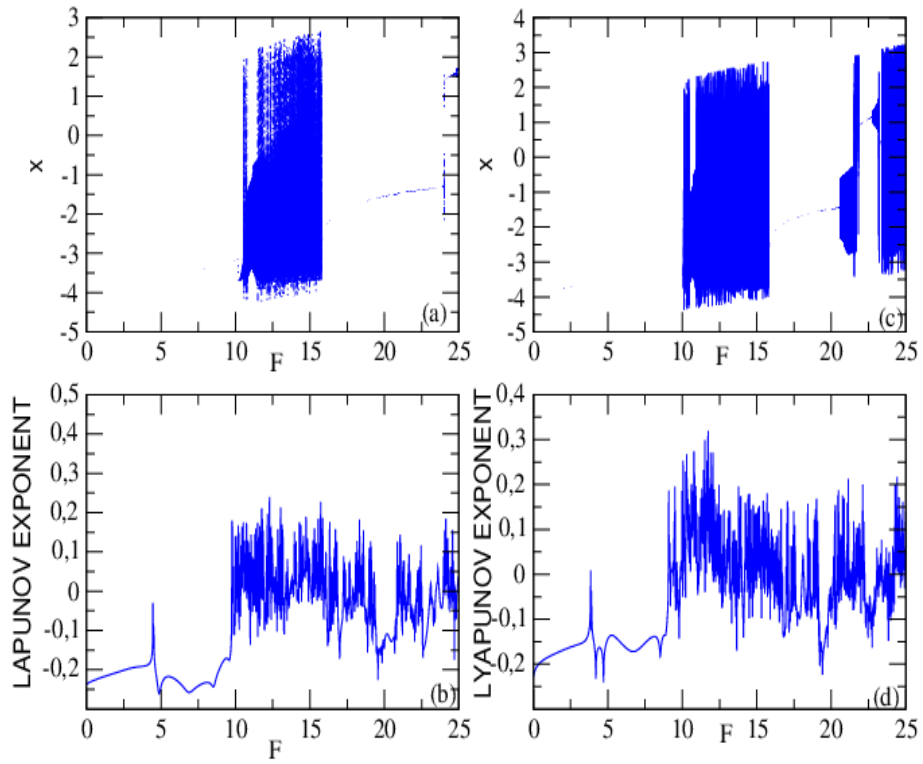


Figure 12: Bifurcation diagram (upper frame) and Lyapunov exponent (lower frame) versus the amplitude  $F$  with the parameters of Figure 11 for  $\beta = 6$ ,  $\alpha = 0$  (left) and  $\alpha = 1$  (right).

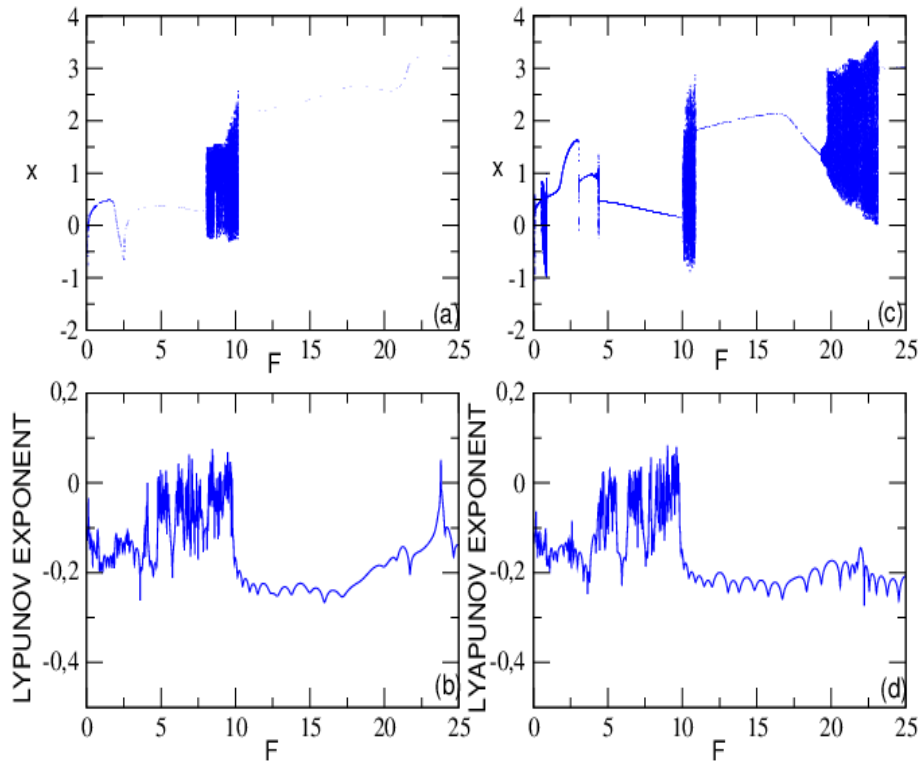


Figure 13: Bifurcation diagram (upper frame) and Lyapunov exponent (lower frame) versus the amplitude  $F$  with the parameters of Figure 11 for  $\beta = 1.80$ ;  $\epsilon = 0.06$ ,  $\alpha = 0$  (left) and  $\alpha = 1$  (right).



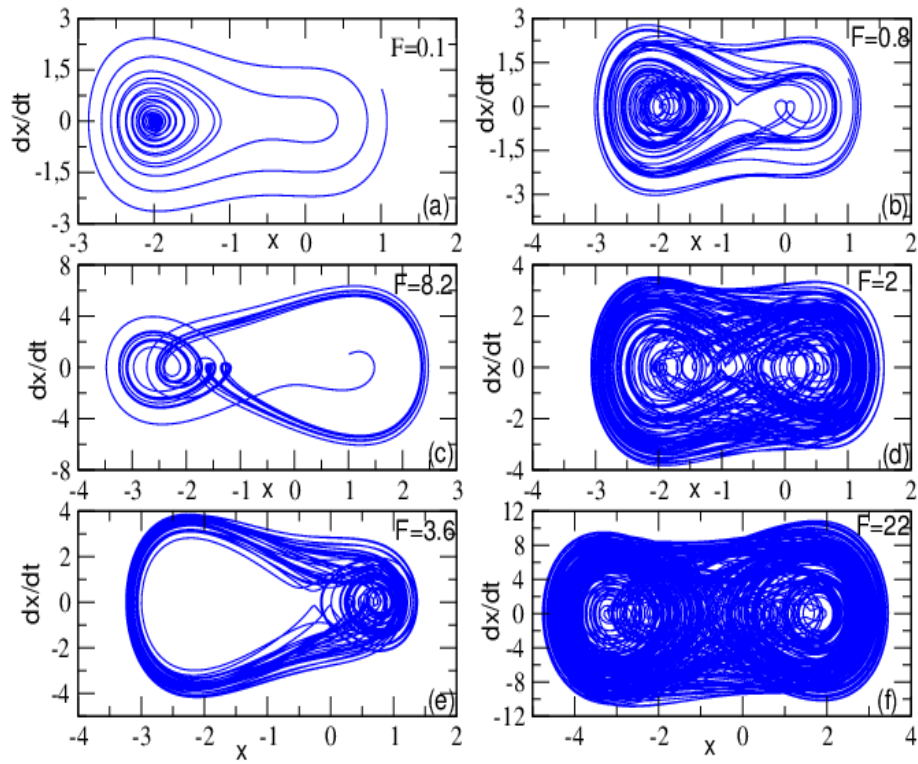


Figure 14: Various phase portraits for several different values of  $F$  with the parameters of Figure 9 and  $\alpha = 0$ .

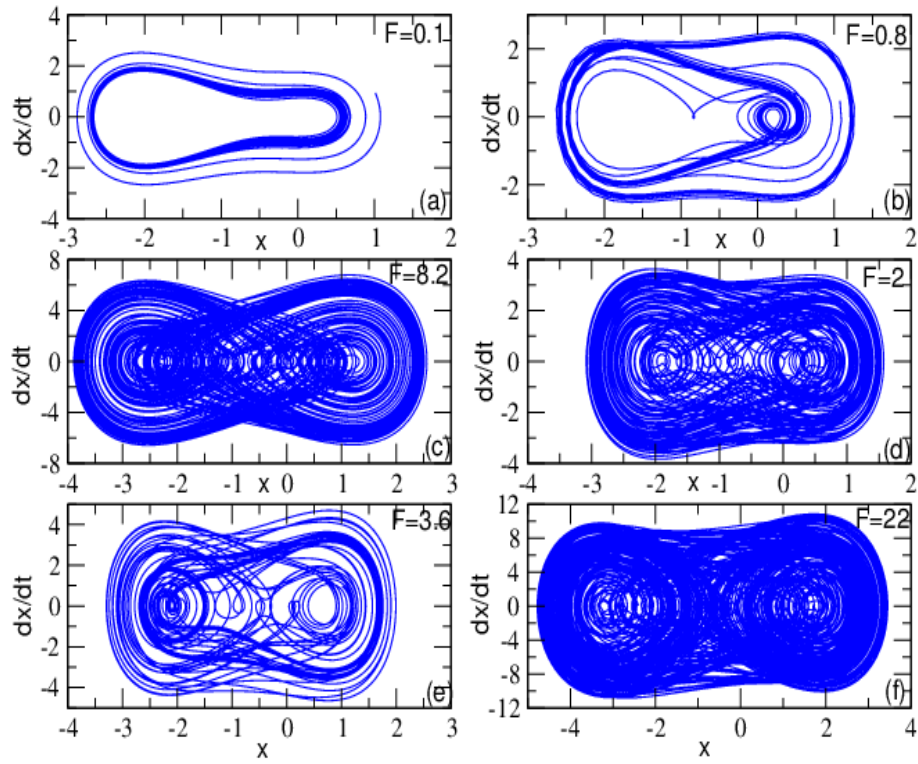


Figure 15: Various phase portraits for several different values of  $F$  with the parameters of Figure 11 and  $\alpha = 1$ .

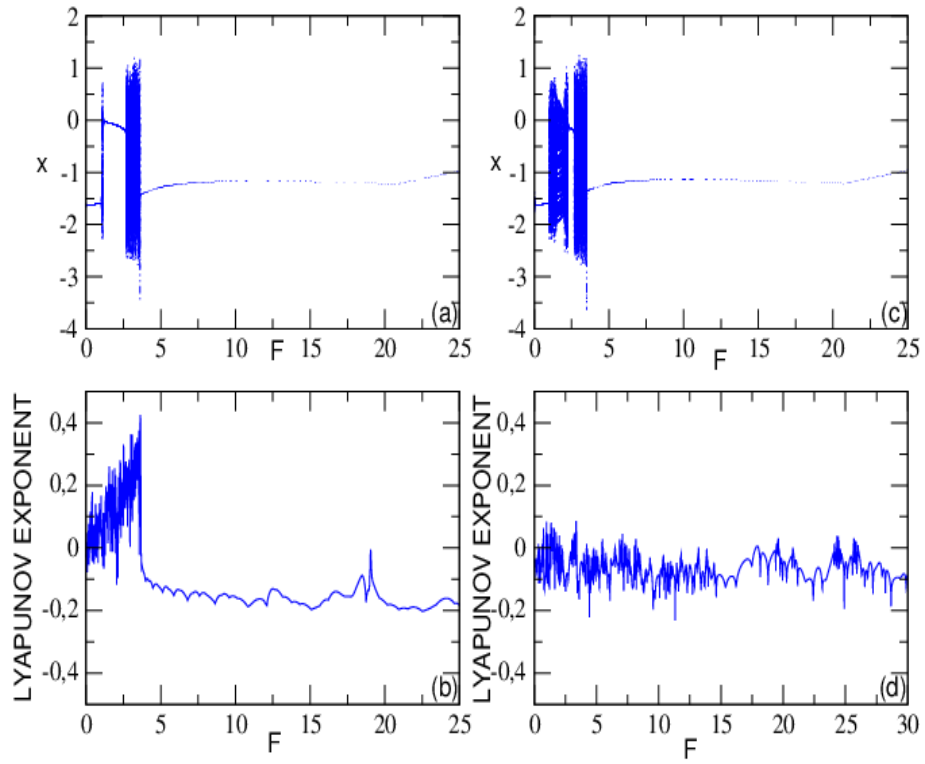


Figure 16: Bifurcation diagram (upper frame) and Lyapunov exponent (lower frame) versus the amplitude  $F$  with the parameters of Figure 11 for  $\Omega = 3$ ,  $\alpha = 0$  (left) and  $\alpha = 1$  (right).

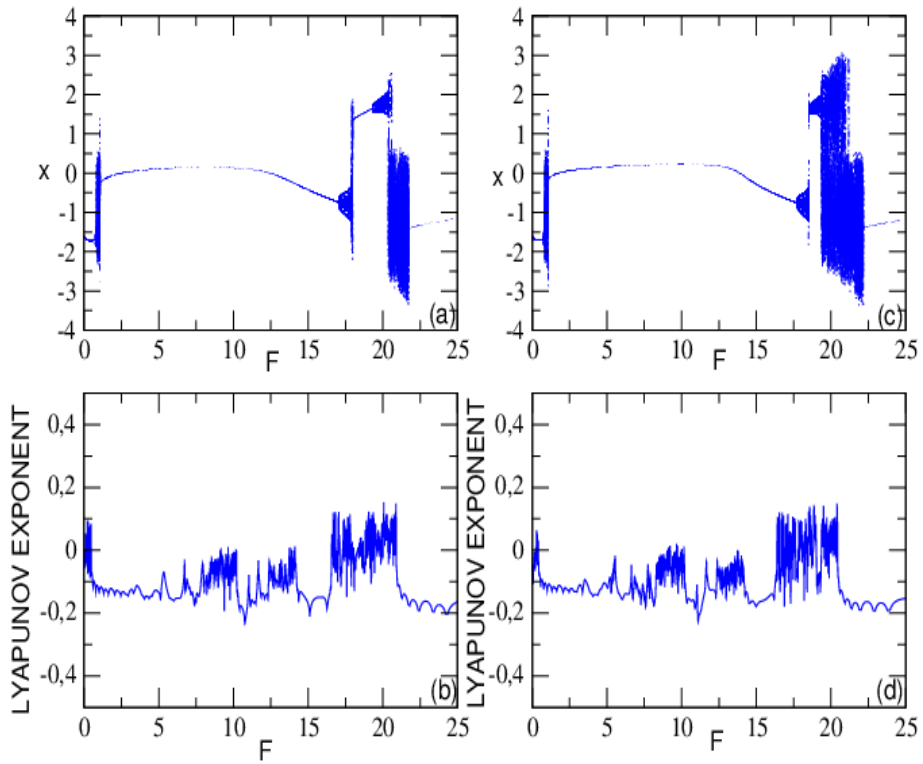


Figure 17: Bifurcation diagram (upper frame) and Lyapunov exponent (lower frame) versus the amplitude  $F$  with the parameters of Figure 11 for  $\Omega = 2$ ,  $\alpha = 0$  (left) and  $\alpha = 1$  (right)..

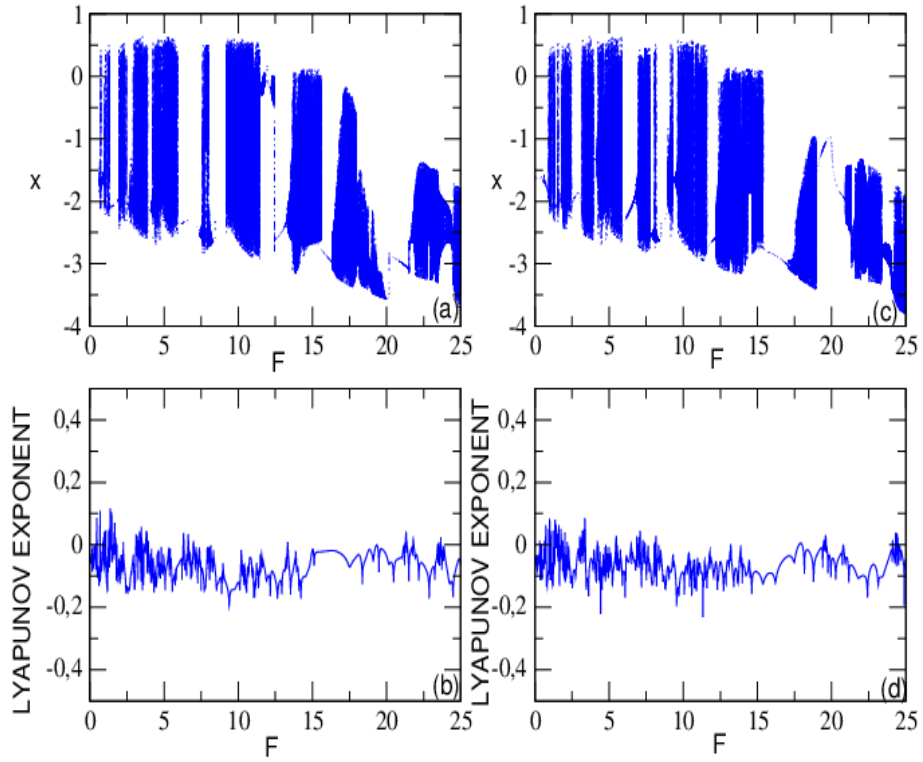


Figure 18: Bifurcation diagram (upper frame) and Lyapunov exponent (lower frame) versus the amplitude  $F$  with the parameters of Figure 11 for  $\Omega = \frac{1}{3}$ ,  $\alpha = 0$  (left) and  $\alpha = 1$  (right).

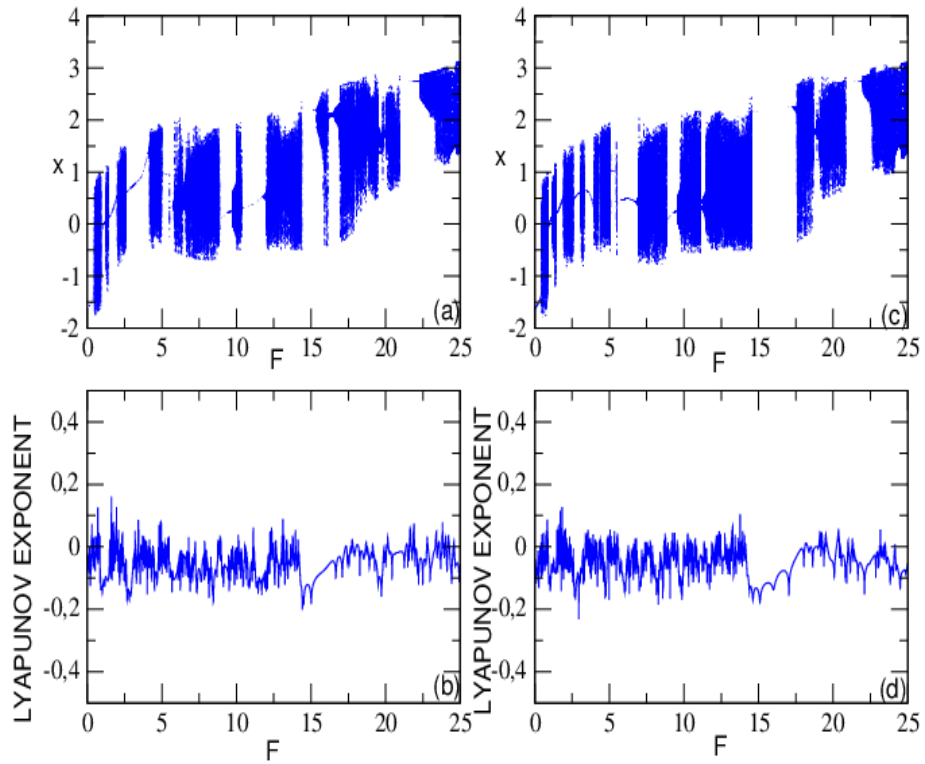


Figure 19: Bifurcation diagram (upper frame) and Lyapunov exponent (lower frame) versus the amplitude  $F$  with the parameters of Figure 11 for  $\Omega = \frac{1}{2}$ ,  $\alpha = 0$  (left) and  $\alpha = 1$  (right).

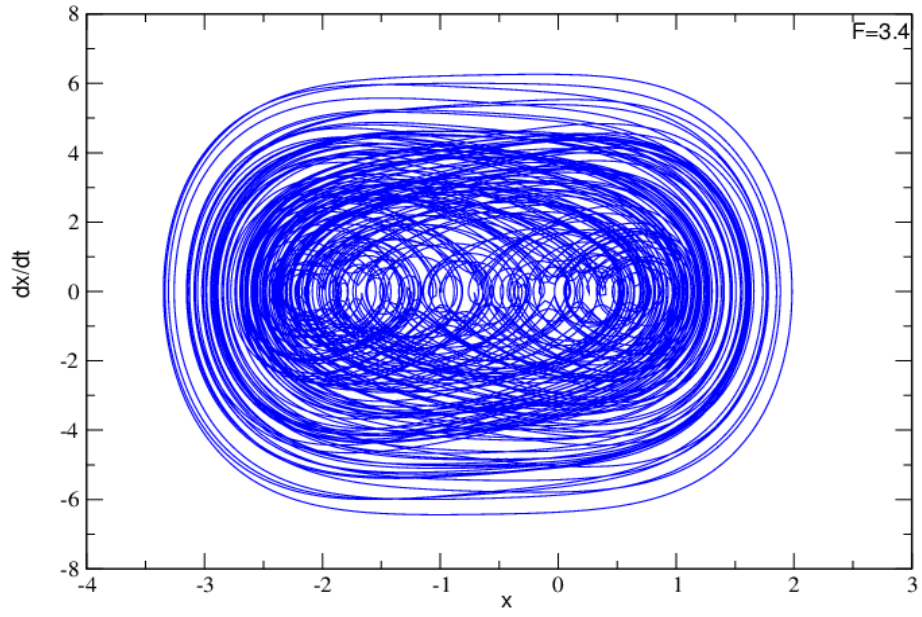


Figure 20: Phase portrait for the first superharmonic resonance with the parameters of Figure 16

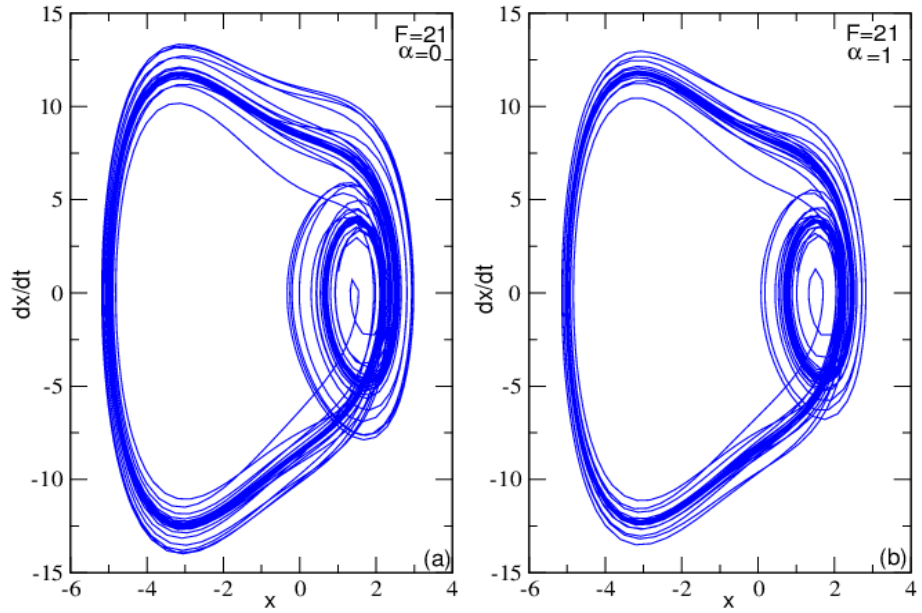


Figure 21: Phase portrait for the second superharmonic resonance with the parameters of Figure 17 .

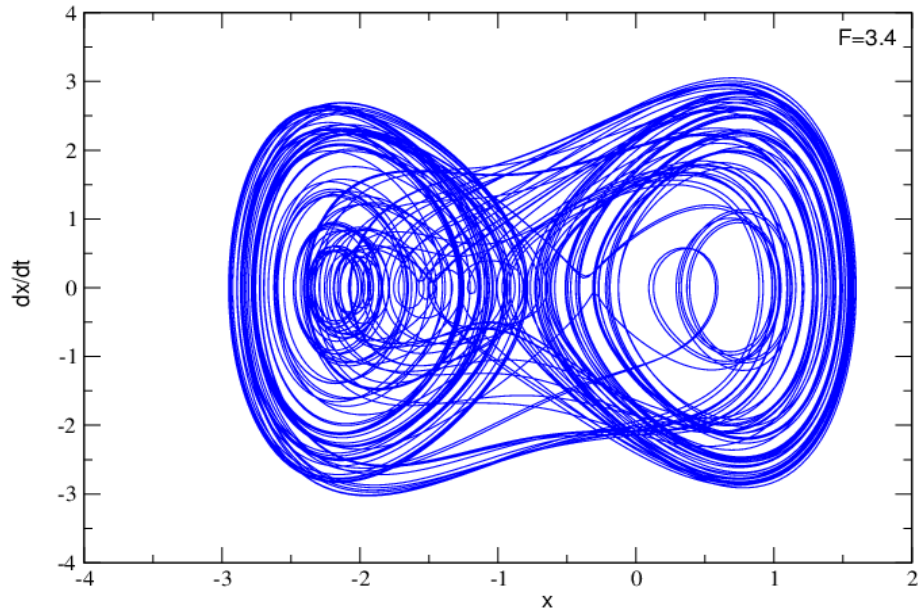


Figure 22: Phase portrait for the first subharmonic resonance with the parameters of Figure 18.

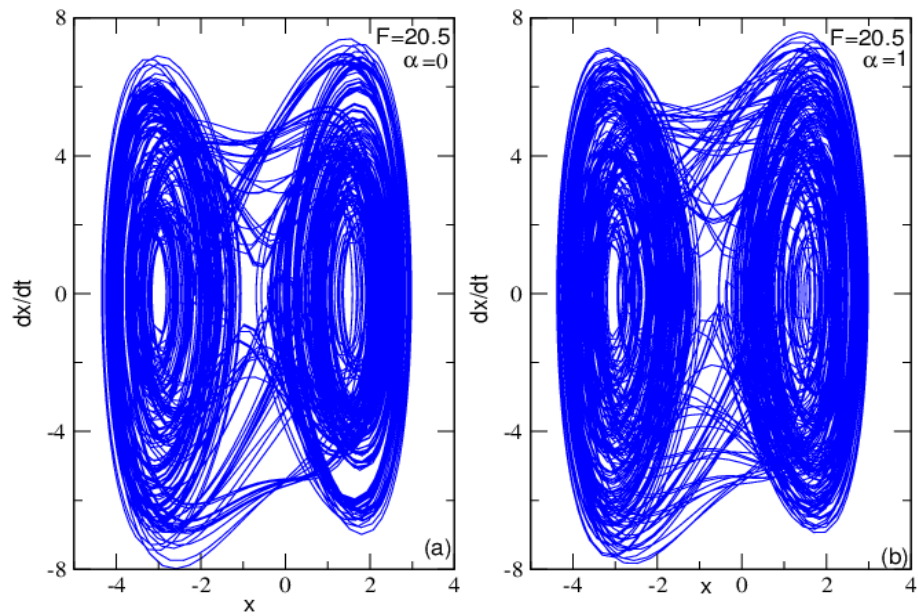


Figure 23: Phase portrait for the second subharmonic resonance with the parameters of Figure 19.



## 6 Conclusion

In this paper, we have studied the nonlinear dynamics of plasma oscillations modeled by forced modified Van der Pol-Duffing oscillator. The model has been described and the corresponding equation of motion obtained. In the harmonic case, the balance method has enabled us to derive the amplitude of harmonic oscillations and the effects of the different parameters on the behaviors of model have been analyzed. For the resonant states case, the response amplitude, stability have been derived using multiple time-scales method and perturbation method it appears the two-order and three-order superharmonic and subharmonic resonances. The effects of different parameters on these resonances are been found and we noticed that the hybrid and pure quadratic parameters have several action on two-order resonances and three-order resonance are affected by the cubic nonlinear parameters. The influences of the dissipative parameter on the resonant, hysteresis and jump phenomena have been highlighted. Our analytical results have been confirmed by numerical simulation. Various bifurcation structures showing different types of transitions from quasi-periodic motions to periodic and chaotic motions have been drawn and the influences of different parameters on these motions have been study. It is noticed that chaotic motions have been controlled by the parameters  $\epsilon$ ,  $\beta$  and  $\gamma$  but also the hybrid quadratic parameter  $\alpha$ . The results show a way to predict admissible values of the signal amplitude for a corresponding set of parameters. This could be helpful for experimentalists who are interested in trying to stabilize such a system with external forcing. Through these studies we notice that the hybrid quadratic term have not neglected in study of nonlinear dynamics of plasma oscillations. For practical interests, it is useful to develop tools and to find ways to control or suppress such undesirable regions. This will be also useful to control high amplitude of oscillations obtained and which are generally source of instability in plasma physics.

## Acknowledgments

The authors thank IMSP-UAC and Benin government for financial support.

## References

- [1] C. Hayashi, *Nonlinear Oscillations in Physical Systems*, (McGraw Hill, New York, 1964), Sec.1.5 .
- [2] A. H. Nayfeh, *Introduction to perturbation techniques*, (John Wiley and Sons, New York, 1981), Sec.4.5.

- [3] J. Guckenheimer and P. J. Holmes, *Nonlinear oscillations, dynamical systems and bifurcations of vectors fields*, (Springer-Verlag, Berlin, New York, 1984), Sec. 1.3.
- [4] S. H. Strogatz, *Nonlinear dynamics and chaos with applications to physics, chemistry and engineering*, (Westview Press, Cambridge, 1994), Sec. 1.2.
- [5] J. D. Murray, *Mathematical biology*, (Third edition, Springer, New York, 2001), pp. 218 – 271.
- [6] G. V. Paeva, *Steath phenomena in dusty plasma*, (PhD thesis, Technische Universiteit Eind-hoven, 2005).
- [7] S. Park, C. R. Seon and W. Choe, *Physics of Plasma* 11, 5095 (2004).
- [8] R. A. Mahaffey, *Physics of Fluids* 19, 1837 (1976).
- [9] K. Ostrikov, *Rev. Mod. Phys* 77, 489 (2005).
- [10] K. Ostrikov and S. Xu, *Plasma-aided Nanofabrication: from Plasma Sources to Nanoassem-bly* (John Wiley Sons, Weinheim, 2007), pp. 149 – 280.
- [11] H. G. Enjieu Kadji, J. B. Chabi Orou and P. Wofo, *Physica Scripta* (In Press) (2007).
- [12] H. G. Enjieu Kadji, B. R. Nana Nbandjo, J. B. Chabi Orou, and P. K. Talla, *Nonlinear dynamics of plasma oscillations modeled by an anharmonic oscillator* (2007).
- [13] B. E. Keen and W. H. Fletcher, *Journal of Physics A: Gen. Phys* 5, 152 (1972).
- [14] B. E. Keen, and W. H. Fletcher, *Plasma Physics* 13, 419 (1970).
- [15] L. H. Li and M. Matsuoka, *Radiophysics and Quantum Electronics* 99, N0.1, 75 (1996).
- [16] J.Loverich and U. Shumlak, *Physics of Plasma* 13, 082310 (2006).
- [17] R. Bhattacharyya and M. S. Janaki, *Physics of Plasma* 13, 044508 (2006).
- [18] U. Shumlak and J. Loverich, *Journal of Computational Physics* 187, 620 (2003).

- [19] T. Kanki, M. Nagata and T. Uyama, *IEEE Transactions on Magnetics* Vol42, N0.4, 1403 (2006).
- [20] M. Arshad Mirza, T. Rafiq and G. Murtaza, *Physics of Plasma* 13, 1107 (1999).
- [21] R. Dendy, *Plasma Physics: an introductory course* (Cambridge University Press 1993), pp. 56, 370.
- [22] H. C. S. Hsuan, *Phys. Rev* 172, 137 (1968).
- [23] V. Land and W. J. Goedheer, *IEEE Trans. Plasma Scie*, 35, 280 (2007).
- [24] Rajasekar S, Parthasarathy S, Lakshmanan M. *Prediction of horseshoe chaos in BVP and DVP oscillators*. *Chaos, Solitons and Fractals* 1992; 2 : 271.
- [25] J. Proud and al., *Plasma Processing of Materials: Scientific Opportunities and Technologies Challenges*. National Academy Press, Washington D.C. (1991).
- [26] N. Piskunov, *Calcul Différentiel et intégral*, Tome II, 9<sup>e</sup> edition, MIR, Moscou (1980).